Hindawi
International Journal of Antennas and Propagation
Volume 2023, Article ID 1339236, 10 pages
https://doi.org/10.1155/2023/1339236

Research Article

A Compact Planar Ultra-Wideband Array Antenna

Junli Zhu, Mengfei Chen, Ziting Li, and Jingping Liu

School of Electronic and Optical Engineering, Nanjing University of Science and Technology, Nanjing 210094, China

Correspondence should be addressed to Jingping Liu; liujingping@njust.edu.cn

Received 17 June 2023; Revised 21 September 2023; Accepted 28 September 2023; Published 10 October 2023

Academic Editor: Anna Pietrenko-Dabrowska

Ultra-wideband (UWB) antennas have recently gained prominence in communication, radar technology, and electronic warfare domains. The quick development of these antennas is due to the wide bandwidth requirements of pulse radar, ground penetrating radar, electromagnetic compatibility, spaceborne communication systems, stealth target detection, and more. Aiming to address the defects of existing UWB antennas, which often have narrow bandwidth and low gain, a planar ultra-wideband microstrip array antenna was designed to achieve good ultra-wideband characteristics and effectively improve the gain of the antenna. The initial bandwidth of the rectangular monopole antenna was 10 GHz–20 GHz. After loading multiple steps on the monopole patch, the bandwidth was increased to between 10 and 38 GHz. Using the new ultra-wideband array method that combines series feed and angle feed and the defective ground structure (DGS), the array maintains the ultrawide bandwidth span of 10–38 GHz of the array element, and the maximum gain of the antenna in the bandwidth was increased from 5.18 dBi to 9.55 dBi. The challenge of impedance matching of antenna units in ultra-wideband is resolved by the novel array technique, which also increases the antenna's gain within the bandwidth. The antenna simulation is consistent with the measurement results. With its extensive operating frequency band, high gain, compactness, and favorable radiation attributes, this newly designed antenna holds significant promise for application in UWB radar systems.

1. Introduction

UWB antennas are integral to UWB radar equipment and are essential microwave devices in UWB wireless systems. The rapid development of ultra-wideband antennas is driven by the wide bandwidth demands of systems such as pulse radar, ground penetrating radar, electromagnetic compatibility, spaceborne communication systems, stealth target detection, and more. As electronics and information technology have advanced, there is a growing trend in the continuous evolution of ultra-wideband antennas towards both miniaturization and broader bandwidth. This area has become a focal point of research in recent years. Due to low manufacturing cost, low profile, compact structure, and wide impedance bandwidth, planar antennas are widely used in the field of ultra-wideband. However, in the antenna design process, in addition to conventional performance indicators such as VSWR and gain, it is also necessary to consider the stability of the antenna pattern, radiation efficiency, and antenna volume, which brings difficulties to the design of ultra-wideband antennas.

Microstrip antennas are favored for their compact dimensions, low profile, and ease of integration. They are widely used in planar antenna arrays. Because the bandwidth of the traditional microstrip antenna is narrow, many scholars have done a lot of research on how to improve the bandwidth of the microstrip antenna, for example, changing the shape of the patch, grounding or slotting the patch, and using a defective structure. In the studies [1–4], U-shaped slot patches, E-shaped patches, air-hole support patches, and stacked patches, respectively, are used to increase patch bandwidth. Majidzadeh et al. [5] designed a quasisquare radiating patch with steps and inserted a rectangular slot and three steps on the ground plane to obtain new resonances and wider bandwidths. Antenna bandwidth is from 2.78 GHz to 19.38 GHz, but the gain in the frequency band

does not exceed 3 dBi. In the study [6], a broadband printed monopole antenna containing a pot radiator fed by coplanar waveguide (CPW) technology is designed. Throughout the whole UWB spectrum, which spans the range of 3 GHz–11 GHz, the planned UWB antenna operates at maximum gain (peak gain 4.1 dBi). To enable the antenna to operate in the 3.1 GHz–10.6 GHz frequency range, the authors in [7] employ a rectangular microstrip patch antenna with truncated corners and arcs. In the frequency band, the antenna's maximum gain is 3.3 dBi. The five-level stepped antenna designed in [8] has a bandwidth ranging from 2.3 GHz to 12.8 GHz, but the gain is only about 3 dBi.

However, monopole microstrip antennas frequently exhibit low gain throughout bandwidth. The array combining of the microstrip antenna elements is also necessary to increase the gain of the UWB antenna. The overall bandwidth of the microstrip antenna array generated by connecting each unit with the microstrip line will be impacted since the microstrip line's own bandwidth is constrained. As a result, it is worthwhile to research how to use a microstrip antenna array to increase gain without significantly decreasing antenna bandwidth.

Series feed structures [9], parallel feed structures [10–19], fractional and Fibonacci arrays [20, 21], and MIMO arrays [22–24] are the most common array architectures used in the current research for planar UWB arrays. The series feed itself possesses limited bandwidth characteristics. To assure the array's bandwidth when using it in the ultra-wideband field, we must extend the feed point into the patch and modify the distance between the feeder and the patch. Three series log-periodic antenna was created in this paper [9]. The 1×9 array among them achieves a total bandwidth of 12.2 GHz between 12.2 GHz and 21.71 GHz, with a bandwidth increase of up to 12.0 dBi. Publications [13] employed a uniplanar compact electromagnetic band gap (UC-EBG) structure and a wideband monopole antenna array. In the working frequency range of 4.5 GHz– 6.5 GHz, the suggested wearable antenna array using parallel feeding may reach a high gain of 11.8 dBi– 13.6 dBi. An 8×8 microstrip array was designed using parallel feeding in this paper [19]. The antenna achieves an impedance bandwidth of 22 GHz–46.3 GHz, obtains the maximum gain of 23.4 dBi in the bandwidth, and excites the antenna elements using microstrip and an H-shaped coupling groove. The fractal and Fibonacci technique is used in this paper [20] to extend the ultra-wideband metamaterial microstrip unit. The antenna bandwidth is increased from 3.37–9.2 GHz to 3.55–10.34 GHz after three iterations. The study in [22] designed a triple band-stop MIMO/diversity ultra-wideband antenna using notched mushroom and electromagnetic bandgap structure technology. The antenna can work in three frequency bands of 3.3–3.6 GHz, 5-6 GHz, and 7.1–7.9 GHz. The zigzag patch makes the perimeter of the patch larger, the impedance matching of the array elements is enhanced, and the coupling between the array elements is improved. The decoupling strip and ground slot structure provide good isolation between the two antennas.

The design described in this paper employs a novel combination of horizontal corner feed and vertical series feed to create an ultra-wideband array antenna. To increase the antenna bandwidth, every element of the array contains several current excitation points that can simultaneously match several different frequency bands. In addition, the performance of the antenna is guaranteed by the fact that the field distribution inside the antenna unit in various frequency bands is unaffected by one another. Moreover, the feed network barely takes up any additional space, making the array efficient and small. In addition, compared to other designs in the aforementioned papers, the ultra-wideband array created in this paper has a wider bandwidth span and a satisfactory gain.

In this paper, an ultra-wideband high-gain array antenna is designed using a stepped ultra-wideband microstrip antenna unit and a new ultra-wideband microstrip array approach. The antenna is compact, has a straightforward design, and offers greater stability and dependability. The impedance bandwidth is realized between 10 GHz and 38 GHz, with a maximum gain of 9.55 dBi. The creation of a brand-new planar ultra-wideband array antenna is discussed in this paper. The antenna's gain and bandwidth are both guaranteed at the same time. The measurement outcomes attest to the intended antenna's good performance.

2. Ultra-Wideband Antenna Unit

The ultra-wideband antenna designed in this paper operates in the band between 10 GHz and 38 GHz, and the ultra-wideband design of the microstrip antenna unit is achieved by loading multiple steps on the rectangular unit. The multilevel stepped structure at the edge of the microstrip patch is a more effective way to expand the bandwidth and reduce the size, and it is also an effective way to achieve ultra-wideband. Since the strong current of the patch is primarily distributed at the edge, processing at the edge of the patch will have a greater impact on the current distribution of the antenna, thus widening its working bandwidth.

Figure 1(a) shows the simulation structure of a rectangular radiation unit. Considering the ultrawide bandwidth of 10 GHz–38 GHz and the radiation efficiency of the antenna, this paper selects the dielectric substrate of the Rogers 5880 model with $\varepsilon_r = 2.2$, $\tan\delta = 0.0009$, and thickness $h = 0.254$ mm. After parameter optimization, the radiation unit size is determined as $w = 7$ mm and $l = 6.5$ mm. The gap distance between the patch and the floor greatly influences the impedance matching. After optimization, the feed line length $l_1 = 5$ mm, the feed line width $w_1 = 0.5$ mm, and the ground plane height $g_l = 4.7$ mm are determined.

The antenna current distribution will be significantly affected by processing the patch's edge, increasing the bandwidth. To increase the antenna bandwidth, this paper uses the loading of 4 steps onto the patch's edge. Figure 1(b) shows the simulation structure of the radiation unit loaded with 4 steps. The antenna step width is optimized, and the optimized antenna dimensions are as follows: the width of the rectangular patch part $w = 7$ mm, the length $l = 6.5$ mm, the feed line length $l_1 = 5$ mm, the feed line width $w_1 = 0.5$ mm, the ground plate width $g_l = 4.7$ mm, the dimensions of all steps are the same, and the side length is 0.5 mm. The overall dimensions of the antenna unit are

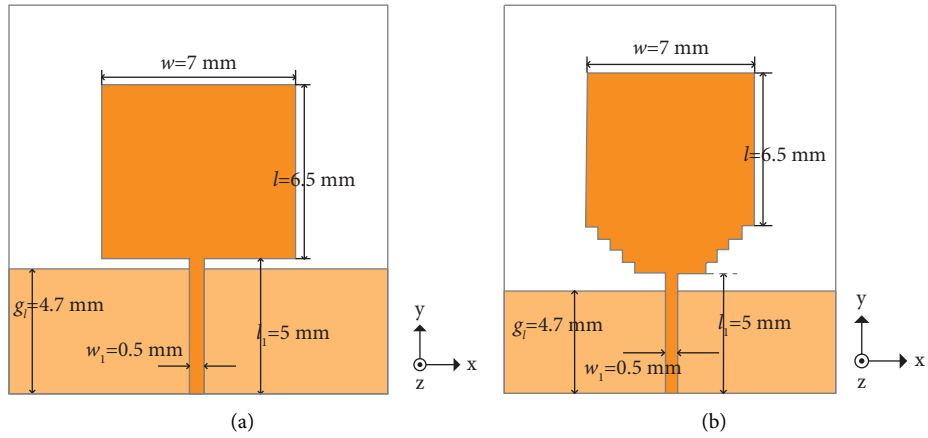

Figure 1: Simulation model: (a) rectangular radiation patch antenna (b) 4-level ladder radiation patch antenna.

16.5 mm × 14 mm. Figure 2 shows the *S*-parameter simulation results for loading a 4-level stepped antenna. The antenna has 5 resonance points, respectively, at 10.8 GHz, 17.7 GHz, 20.1 GHz, 28.6 GHz, and 36 GHz. And the antenna bandwidth range is 10 GHz– 20 GHz. The frequencies of the 5 resonance points correspond to each step size of the antenna. The 4-level stepped antenna's current distribution for each frequency point is shown in Figure 3. As can be observed, the patch's edge and the feeder are where the current is most evenly spread. Because the current distribution and working model alters significantly as the frequency changes, the antenna's pattern and impedance also varies proportionally, which brings challenges to the impedance matching of ultra-wideband antenna elements.

Figure 4 shows the slices of the gain at different frequency points on the *E*-plane (*yoz* plane) and *H*-plane (*xoz* plane) of the 4-level stepped antenna unit. The maximum gain of the radiation unit at each frequency point is shown in Table 1. The maximum gain of the antenna within the operating band at each frequency point is above 3 dBi, with good overall performance.

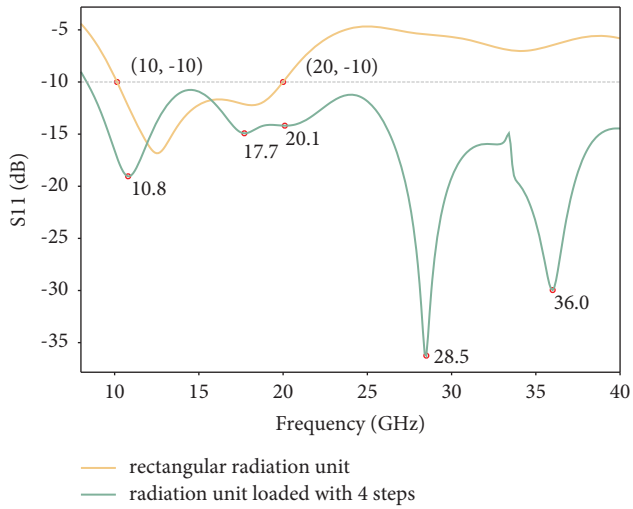

Figure 2: *S*-parameters of rectangular radiation unit and 4-level ladder element antenna.

3. Ultra-Wideband Antenna Array

The average gain of a monopole antenna is only 3–5 dBi, while it can provide basic transmission and reception, it usually falls short of the requirements of a radio system. To increase the gain and enhance its directivity, forming an array is often necessary. As mentioned above, due to the large frequency band span of the UWB unit designed in this paper, the internal field distribution and working model change significantly with frequency, and the port impedance will fluctuate to a certain extent, which brings challenges for the composition of ultra-wideband arrays. In order to solve this problem, a new composition method of UWB array is proposed. Using a feeder with a fixed width at a single feed point will limit its bandwidth, so the author chose a combination of series feed and corner feed, so that the array element has multiple feed points for feeding. Furthermore, the length, width, and impedance of the feeder at the ladder's top and the patch's corner vary. This variation is designed to match the patch's impedance at different ports across multiple frequency bands, thereby guaranteeing the array's bandwidth. The impedance matching between the array element and the feeder is realized by adjusting the distance between the feeder elements and the width of the feeder. The proposed ultra-wideband array improves the gain of the antenna and solves the problem of low gain of the existing wideband antenna. Figure 5 displays the model for the antenna simulation.

A radiation patch loaded with four steps was used as the radiation unit. In the longitudinal direction, the feeding method of series feeding is adopted, and the patches are connected by a microstrip line with a length of l_6 and a width of w_6. The longitudinal spacing of the patches is one-half of the wavelength of the medium corresponding to the center frequency of the antenna. The corner feeding mode is adopted in the transverse direction. The patches are connected with a feeder line of width w_7. The initial value of patch lateral spacing l_7 is half of the wavelength of the medium corresponding to the center frequency of the antenna.

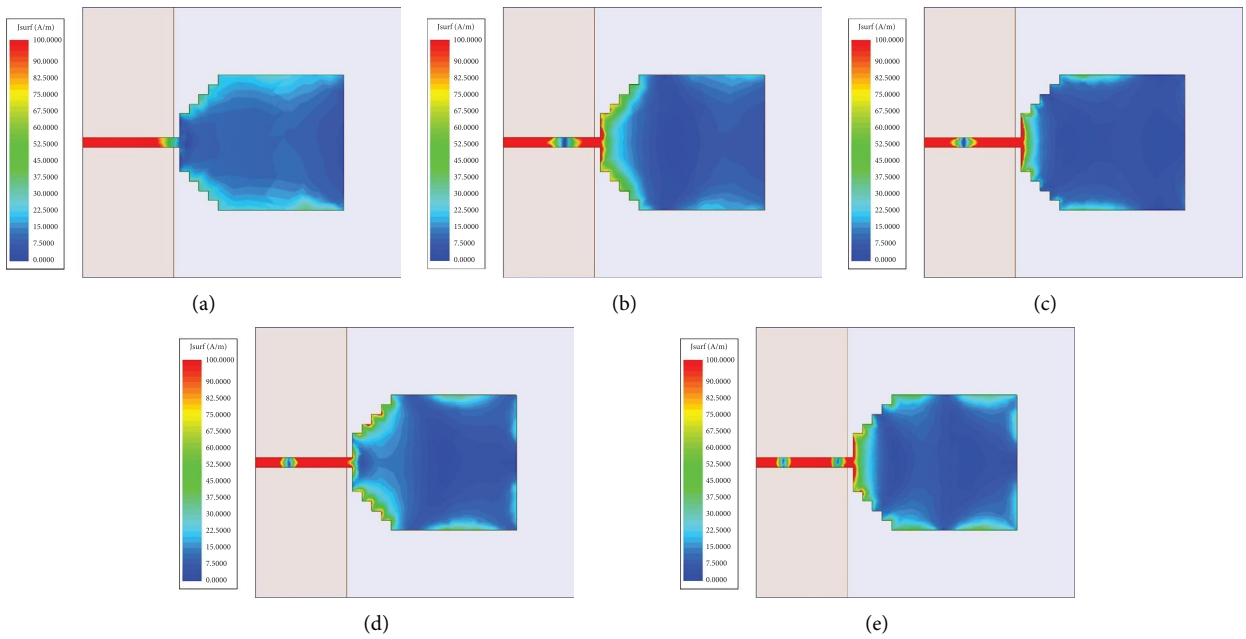

Figure 3: Current distribution of 4-level stepped antenna: (a) 10 GHz, (b) 17 GHz, (c) 24 GHz, (d) 31 GHz, and (e) 38 GHz.

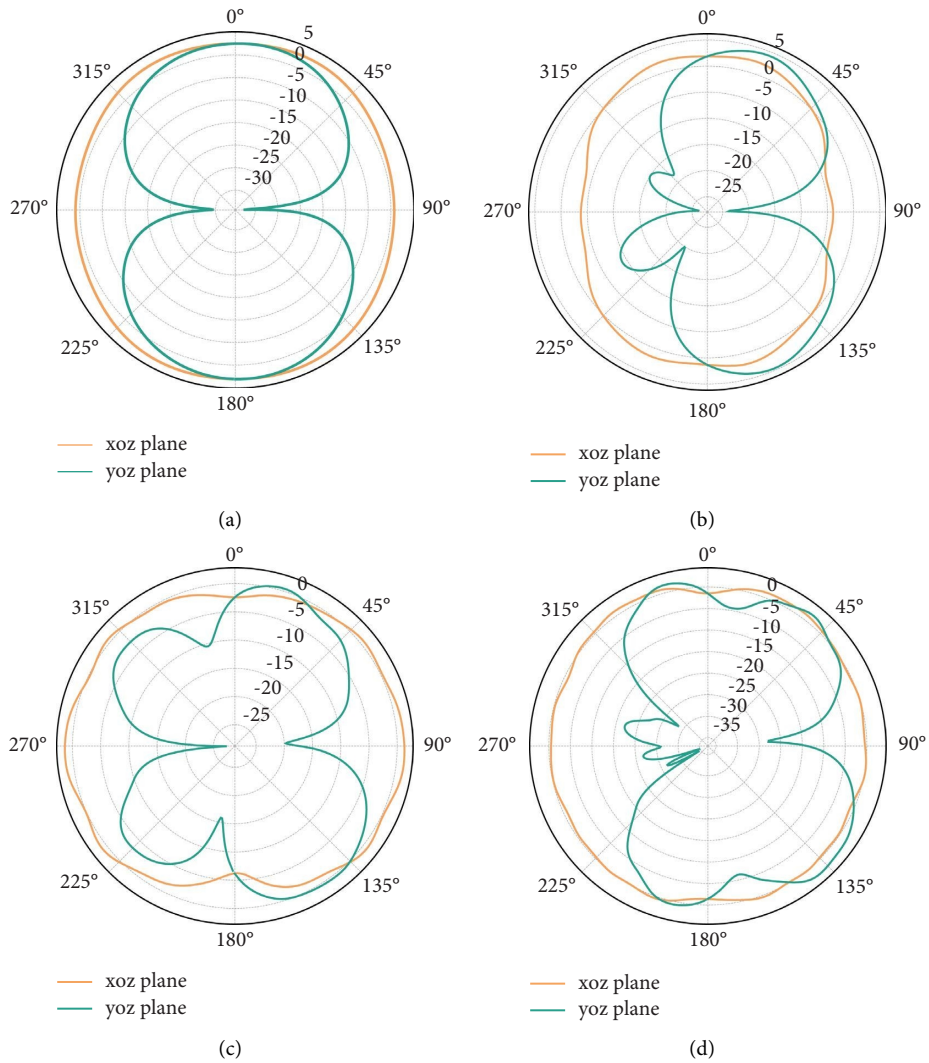

Figure 4: Continued.

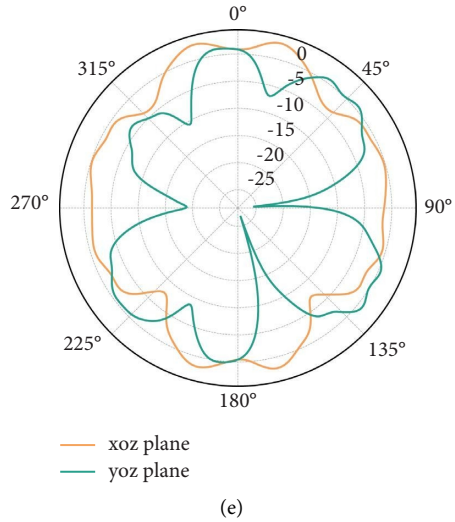

(e)

Figure 4: Gain of 4-level stepped antenna: (a) 10 GHz, (b) 17 GHz, (c) 24 GHz, (d) 31 GHz, and (e) 38 GHz.

Table 1: The maximum gain of the radiation unit loaded with four steps at each frequency point.

Frequency (GHz)	10	17	24	31	38
Maximum gain (dBi)	3.33	4.8	4.68	5.18	4.59

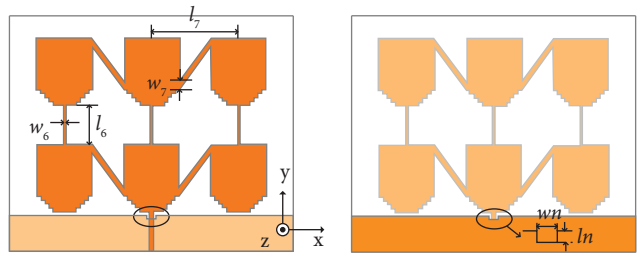

(a) (b)

Figure 5: Simulation model of 2 × 3 UWB array antenna: (a) front side and (b) back side.

Model and simulate the antenna as shown in Figure 5. The simulation analysis of the patch transverse spacing l_7 is carried out. To study the impact of corner-fed microstrip line on the antenna resonant frequency and pattern, change the transverse spacing l_7 from 9 to 13 mm in steps of 1 mm.

Figure 6 shows the change of resonant frequency and S-parameters of the antenna with the transverse spacing of the patch l_7. With the increase of the spacing l_7, each resonant point gradually shifts to the low frequency direction. Among which, the first and second resonant points tend to fuse. The S-parameter value of the third resonant point gradually decreases. The return loss of the fourth resonant point is between −20 dB and −30 dB. After extensive analysis, it was determined that the transverse spacing l_7 should be 11 mm because, when l_7 is small, the antenna does not resonate in the frequency range of 10 GHz–20 GHz and the impedance is not matched, and when l_7 is large, the pattern is poor.

The width of the corner-fed microstrip line w_7 was determined to be 1 mm, the length of the series-fed microstrip line l_6 to be 5 mm, and the width of the feed line w_6 to be 0.3 mm using the same method that was used to simulate the transverse spacing l_7.

4. The Effect of DGS on Antenna Performance

The gap distance between the patch and the floor is crucial for impedance matching. However, as the number of radiating parts increases, simply changing the ground plate's size to alter the distance between the patch and the ground will not be sufficient to modify the impedance matching of the entire antenna. Therefore, this paper improves the grounding plate. A rectangular slit with width wn and length ln is opened for the ground plate, and the current distribution near the ground plate is changed by using the defective ground structure to improve the matching of the antenna. The DGS of the antenna is marked with an ellipse in Figure 5. The diagram below displays the results of the simulation analysis.

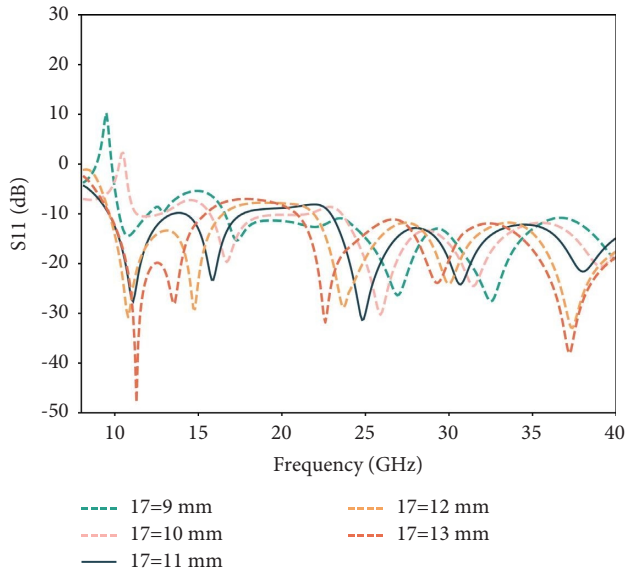

Figure 6: Variation of resonant frequency and *S*-parameters with the transverse spacing l_7.

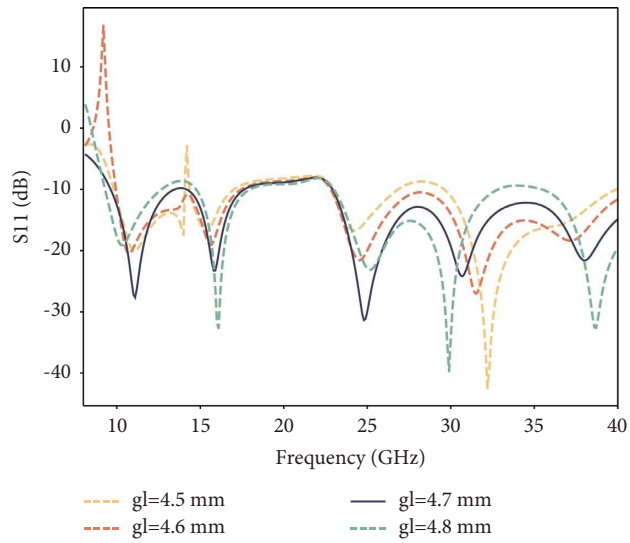

Figure 7: Effects of ground plate width *gl* on antenna impedance matching without slotting.

Figure 7 shows that the effect of changing the ground plane width *gl* on the impedance matching in the frequency range of 17 GHz–23 GHz is relatively minimal when no slot is created. After carving a tiny rectangular groove on the ground plate, the distributed capacitance and distributed inductance are modified to provide the band-pass characteristic in the aforementioned frequency range. Figure 8 clearly shows that the *S*11 value after slotting is lower than that without slotting in the 17 GHz–23 GHz frequency band. The matching impact of this frequency band improves as the length of the slot *ln* increases, but it also causes the matching of higher frequency bands to deteriorate. Through simulation, it was found that the length of the rectangular slot should be 0.3 mm.

The antenna's *Q* value will be slightly lower after slotting, and the antenna's impedance matching needs to be reoptimized. After making the necessary adjustments to place size and impedance matching, the following antenna simulation results are attained.

The size of the optimized array antenna is 36 mm × 30 mm. Figure 9 displays the UWB array antenna's *S*11 simulation results. The antenna resonates at the following four frequencies: 11.3, 15.7, 24.1, and 31.2 GHz. Compared with the radiating element, the resonant frequency of the array antenna changes. This is due to the antenna's current distribution being altered when the ground plate is cut and the radiating units are connected using the series feeder and corner feeder, which changes where the strong current is located on the ladder and shifts the resonance frequency. The impedance bandwidth of the antenna, which still covers 10 GHz–38 GHz, remains unaltered after the array is created.

The comparison of the maximum gain of the UWB antenna unit and array at each frequency is shown in Figure 10. As shown in Table 2, the maximum gain of the

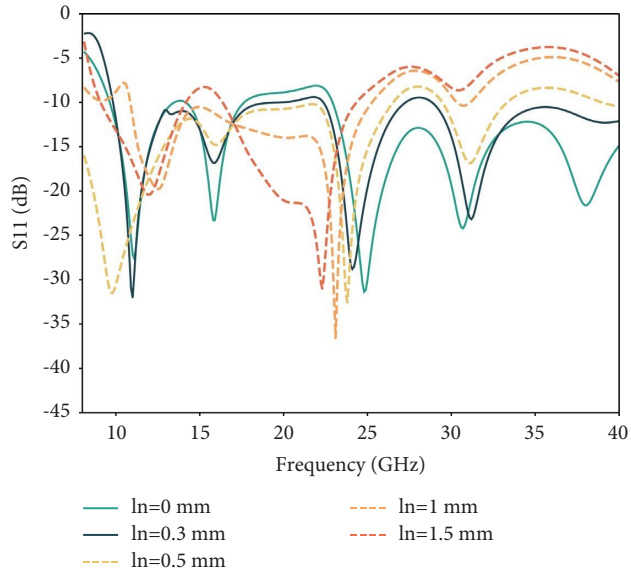

Figure 8: Effects of slot width *ln* on antenna impedance matching when slotting.

UWB array antenna at 10 GHz, 17 GHz, 24 GHz, 31 GHz, and 38 GHz is significantly higher than that of the radiation unit. The antenna achieves the effects of increasing gain and enhancing directivity. Meanwhile, in the design of the array, there are two ways to feed the array elements. The radiating elements are directly connected by the series feeder and the corner feeder, which reduces the antenna size and realizes the antenna's miniaturization design. The array antenna *E*-plane (*yoz* plane) and *H*-plane (*xoz* plane) gain slices at different frequency points are shown in Figure 11. Figure 12 shows the radiation efficiency of the antenna unit and the array, both of which are in the range of 0.8-0.9.

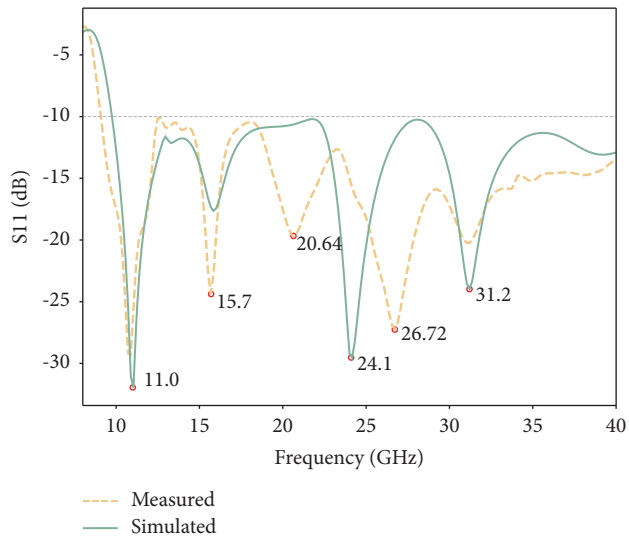

Figure 9: Simulation and measurement results of the 2×3 UWB array antenna's S-parameter.

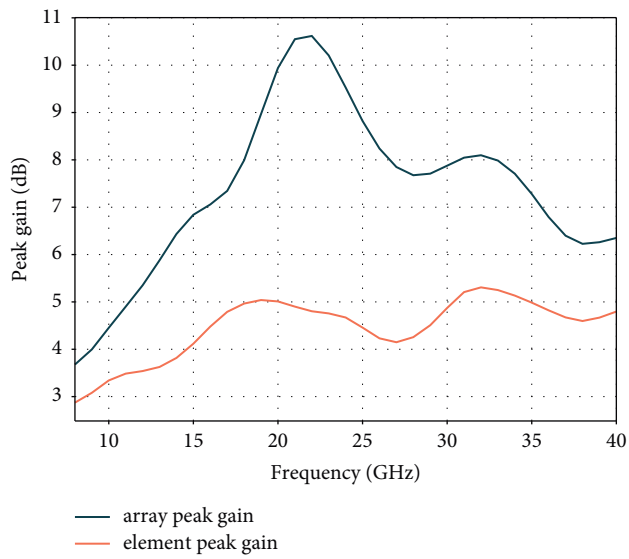

Figure 10: Simulation results of UWB unit and array peak gain.

Table 2: Measured and simulated results of the gain at each frequency point of the 2×3 UWB array antenna.

Frequency (GHz)	10	17	24	31	38
Simulated maximum gain (dBi)	4.45	7.3	9.55	8.07	6.26
Measured maximum gain (dBi)	4.33	6.95	9	7.76	5.4

5. Measurement and Analysis of UWB Array Antenna

The designed array antenna is manufactured. The substrate of the antenna is made of Rogers 5880 plate with a thickness of 0.254 mm, which is consistent with the simulation model. A suitable microwave coaxial connector is then soldered at the antenna feed point. Figure 13(a) shows the physical appearance of the $36 \times 30\ \text{mm}^2$ UWB array antenna for the frequency range of 10 GHz–38 GHz. Figure 9 presents the measurement results. According to the measurement results, the antenna exhibits 5 resonance points between 10 GHz and 38 GHz. The simulation results correspond to the first resonance point (11 GHz), second resonance point (15.7 GHz), and fifth resonance point (31.2 GHz), while the third and fourth resonance points emerge from the third resonance point (24.1 GHz) in the simulation results. In actuality, the radiating unit loaded with four steps should potentially create five resonance points, according to the design principle. But after the grounding plate is slit and each radiating unit is connected by a series feeder and a corner feeder, the antenna's current distribution is altered, and the position of

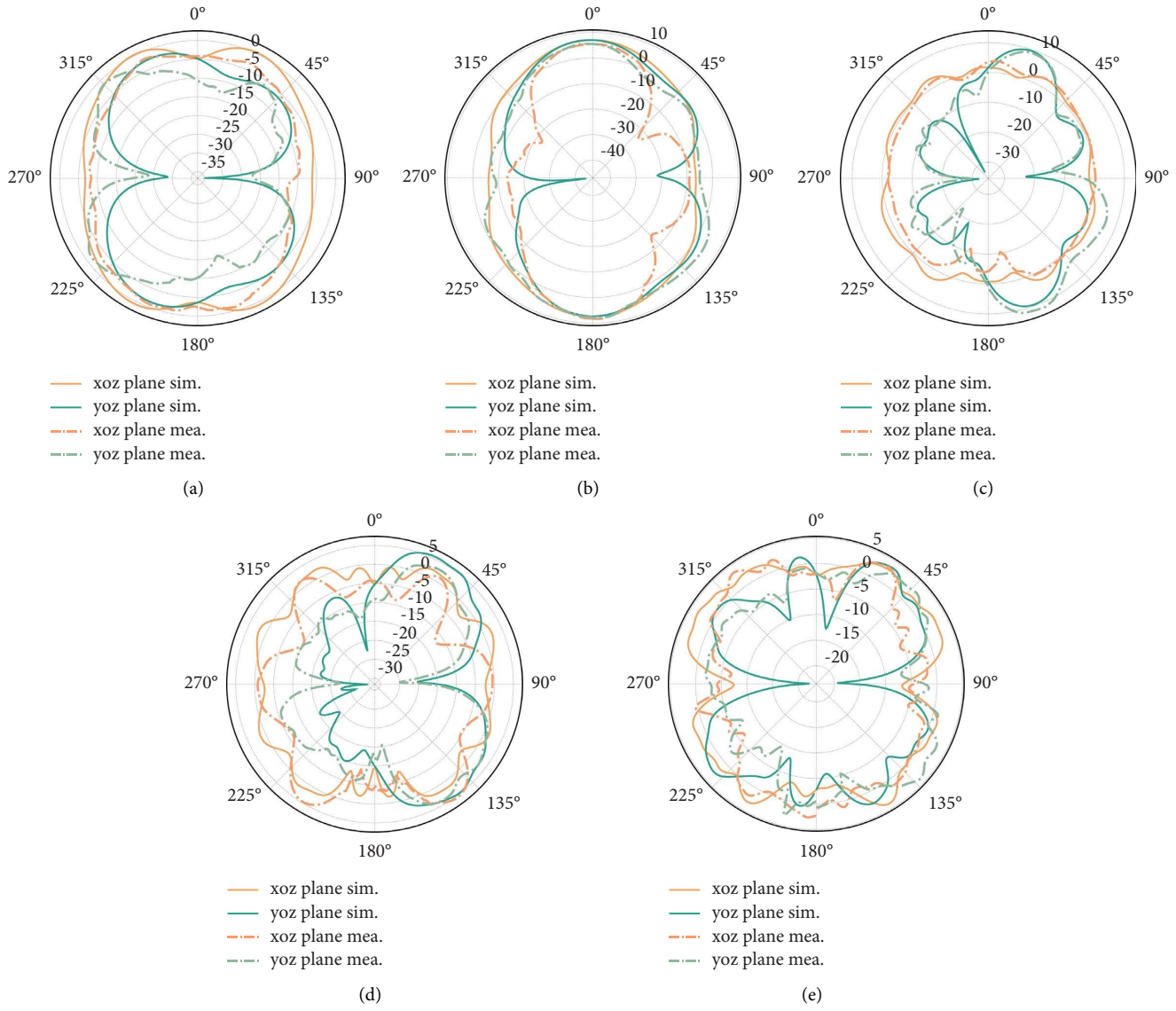

Figure 11: Gain of UWB array antenna: (a) 10 GHz, (b) 17 GHz, (c) 24 GHz, (d) 31 GHz, and (e) 38 GHz.

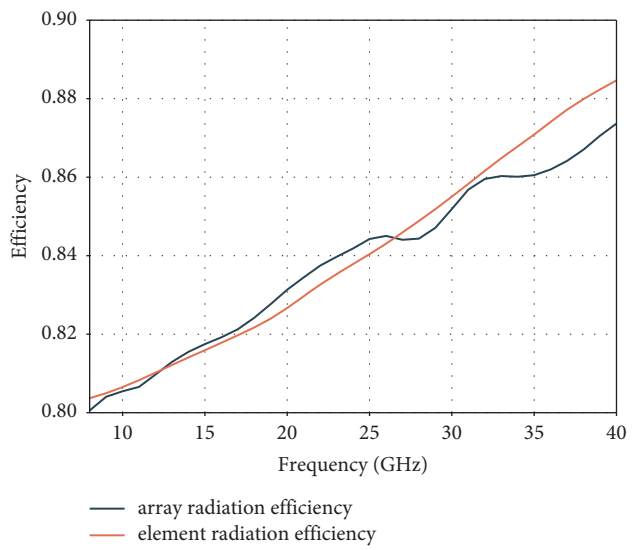

Figure 12: Radiation efficiency of antenna unit and array.

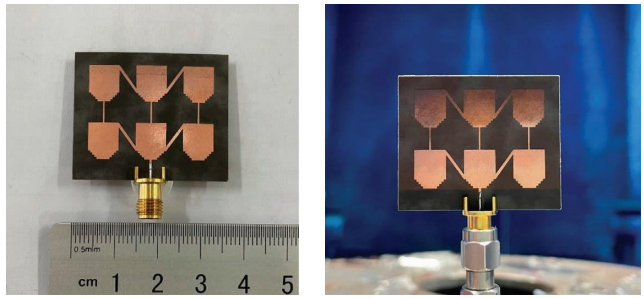

(a) (b)

Figure 13: (a) 10 GHz–38 GHz UWB array antenna physical appearance. (b) Photo of the array antenna measured in a microwave anechoic chamber.

the strong current shifts, resulting in the combination of the third and fourth resonance points into a single point during simulation.

The antenna gain is measured using the comparison method. Maintain the same receiving antenna location, transmitting antenna power, and transmitting antenna position. Both the measurement antenna and the standard antenna with known gain are employed as receiving antennas, and the power they receive is measured. The gain of the measurement antenna can be calculated based on the principle that the power density close to the receiving antenna stays constant. The gain on the *E*- or *H*-plane can then be determined by rotating the antenna along its *E*- or *H*-plane. Measure the gain of the antenna at five frequency points of 10 GHz, 17 GHz, 24 GHz, 31 GHz, and 38 GHz, respectively. Table 2 shows the simulation and measurement comparison of the peak gain. Figure 13(b) is a photo of the ultra-wideband array during gain measurement in a microwave anechoic chamber. Figure 11 compares the *E*-plane (*yoz* plane) and *H*-plane (*xoz* plane) gain slices of the array antenna measured and simulated at various frequencies. There is a lot of noise at 38 GHz since the equipment being used is getting close to its maximum measurement frequency limit, making the measured gain curves appear unsmooth. In addition, the actual gain is slightly less than the simulation because of the testing loss, but the overall trend is consistent with the simulation results.

6. Conclusions

This paper describes the design process of planar UWB antenna arrays. The UWB antenna unit is designed first. The antenna unit's bandwidth is increased from 10–20 GHz to 10–38 GHz by loading multilevel steps on a conventional rectangular microstrip patch and altering the current distribution at the patch's edge. The UWB elements are then assembled into arrays. The array uses a series feed mode longitudinally and the corner feed method transversely. The longitudinal and transverse array element spacing and feeder width are adapted, and the defective ground structure is used to adjust and optimize the performance of the array. As a result, the maximum gain of the ultra-wideband antenna array at 10 GHz, 17 GHz, 24 GHz, 31 GHz, and 38 GHz reaches 4.45 dBi, 7.30 dBi, 9.55 dBi, 8.07 dBi, and 6.26 dBi, respectively, which is a significant improvement compared to ultra-wideband units. Finally, the designed antenna is processed and measured, and the empirical results validate the correctness of the design method, and the antenna exhibits good performance.

Data Availability

The data used to support the findings of this study are available from the corresponding author upon request.

Conflicts of Interest

The authors declare that there are no conflicts of interest regarding the publication of this paper.

Acknowledgments

This work was supported by the National Natural Science Fund (61871442), Science and Technology on Electromechanical Dynamic Control Laboratory, China, no. 6142601200504, and Ministries Fund (2020-JCJQ-JJ-397) funding.

References

[1] J. Xu, W. Hong, Z. H. Jiang, and H. W. Zhang, "Low-profile patch array antenna with corporate stacked microstrip and substrate integrated waveguide feeding structure," *IEEE Transactions on Antennas and Propagation*, vol. 67, no. 2, p. 6, 2019.

[2] J. Xu, W. Hong, Z. H. Jiang, H. Zhang, and K. Wu, "Low-profile wideband vertically folded slotted circular patch array for *ka* band applications," *IEEE Transactions on Antennas and Propagation*, vol. 68, no. 9, pp. 6844–6849, 2020.

[3] Y. Li and K.-M. Luk, "60-GHz substrate integrated waveguide fed cavity-backed aperture-coupled microstrip patch antenna arrays," *IEEE Transactions on Antennas and Propagation*, vol. 63, no. 3, pp. 1075–1085, 2015.

[4] M. Khalily, R. Tafazolli, P. Xiao, and A. A. Kishk, "Broadband mm-wave microstrip array antenna with improved radiation characteristics for different 5G applications," *IEEE Transactions on Antennas and Propagation*, vol. 66, no. 9, pp. 4641–4647, 2018.

[5] M. Majidzadeh, C. Ghobadi, J. Nourinia, and J. Poorahmadazar, "Small monopole antenna with modified slot ground plane for

UWB applications," in *Proceedings of the 20th Iranian Conference on Electrical Engineering (ICEE2012)*, pp. 1078–1082, IEEE, Tehran, Iran, May 2012.

[6] S. Ahmad, U. Ijaz, S. Naseer et al., "A jug-shaped CPW-fed ultra-wideband printed monopole antenna for wireless communications networks," *Applied Sciences*, vol. 12, no. 2, p. 821, 2022.

[7] N. Mishra and S. Beg, "A miniaturized microstrip antenna for ultra-wideband applications," *AEM*, vol. 11, no. 2, pp. 54–60, 2022.

[8] K. Vprashanth, A. Tejasri, K. Sandeep, U. Sateesh Kumar, G. Swarupa, and G. Swarupa, "Design of UWB antenna with WLAN & X-band notch for wireless communication," *International Journal of Engineering & Technology*, vol. 7, no. 2.7.7, p. 484, 2018.

[9] T. Varum, J. Caiado, and J. N. Matos, "Compact ultra-wideband series-feed microstrip antenna arrays for IoT communications," *Applied Sciences*, vol. 11, no. 14, p. 6267, 2021.

[10] Z. Fang, H. Yang, Y. Gao et al., "Design of a 2-bit reconfigurable UWB planar antenna array for beam scanning application," *IEEE Open Journal of Antennas and Propagation*, vol. 4, pp. 91–96, 2023.

[11] V.-T. Nguyen and J.-Y. Chung, "Design of a planar antenna array with wide bandwidth and narrow beamwidth for IR-UWB radar applications," *Applied Sciences*, vol. 12, no. 17, p. 8825, 2022.

[12] M. Garbaruk, "A planar four-element UWB antenna array with stripline feeding network," *Electronics*, vol. 11, no. 3, p. 469, 2022.

[13] H. Zu, B. Wu, P. Yang, W. Li, and J. Liu, "Wideband and high-gain wearable antenna array with specific absorption rate suppression," *Electronics*, vol. 10, no. 17, p. 2056, 2021.

[14] S. Ahmed, T. Kim Geok, M. Y. Alias et al., "A UWB antenna array integrated with multimode resonator bandpass filter," *Electronics*, vol. 10, no. 5, p. 607, 2021.

[15] Y. Wang, F. Zhu, and S. Gao, "Design and implementation of connected antenna array for ultra-wide applications," *Progress in Electromagnetics Research C*, vol. 58, pp. 79–87, 2015.

[16] Y. K. Choukiker, S. K. Behera, and S. K. Sharma, "Two and four-element wideband sectoral fractal array antennas with omni-directional radiation patterns," in *Proceedings of the 2013 IEEE Applied Electromagnetics Conference (AEMC)*, pp. 1-2, Bhubaneswar, India, December 2013.

[17] Y.-Y. Yang and Q.-X. Chu, "Planar 4-element UWB antenna array and time domain characterization," *Microwave and Optical Technology Letters*, vol. 50, no. 12, pp. 3118–3123, 2008.

[18] H.-Z. Liu, J. C. Coetzee, and K. Mouthaan, "UWB antenna array for wireless transmission along corridors," *Microwave and Optical Technology Letters*, vol. 50, no. 4, pp. 886–890, 2008.

[19] Q. Tan, K. Fan, Y. Yu, C. Yin, and G. Luo, "Ultra-wideband planar patch antenna array using multimode resonant antenna element for millimeter-wave applications," *Microwave and Optical Technology Letters*, vol. 65, no. 1, pp. 320–327, 2023.

[20] B. R. Shookooh, A. Monajati, and H. Khodabakhshi, "Theory, design, and implementation of a new family of ultra-wideband metamaterial microstrip array antennas based on fractal and Fibonacci geometric patterns," *J Electromagn Eng Sci*, vol. 20, no. 1, pp. 53–63, 2020.

[21] B. Rezaei Shookooh, A. Monajati, and H. Khodabakhshi, "Ultra-wideband metamaterial-loaded microstrip array antennas using Fibonacci & fractal geometric patterns, design and modelling," *EJECE*, vol. 4, no. 5, 2020.

[22] N. Jaglan, S. D. Gupta, E. Thakur, D. Kumar, B. K. Kanaujia, and S. Srivastava, "Triple band notched mushroom and uniplanar EBG structures based UWB MIMO/diversity antenna with enhanced wide band isolation," *AEU International Journal of Electronics and Communications*, vol. 90, pp. 36–44, 2018.

[23] N. Jaglan, S. D. Gupta, B. K. Kanaujia, and M. S. Sharawi, "10 element sub-6-GHz multi-band double-T based MIMO antenna system for 5G smartphones," *IEEE Access*, vol. 9, pp. 118662–118672, 2021.

[24] N. Jaglan, S. D. Gupta, and M. S. Sharawi, "18 element massive MIMO/diversity 5G smartphones antenna design for sub-6 GHz LTE bands 42/43 applications," *IEEE Open Journal of Antennas and Propagation*, vol. 2, pp. 533–545, 2021.